Preprints of the 19th World Congress
The International Federation of Automatic Control
Cape Town, South Africa. August 24-29, 2014

Impedance Control of a Rotary Series Elastic Actuator for Knee Rehabilitation

Wilian M. dos Santos and Adriano A. G. Siqueira

Engineering School of São Carlos, University of São Paulo. Center for Robotics of São Carlos and Center for Advanced Studies in Rehabilitation, São Paulo, Brazil (e-mail: wilianmds@sc.usp.br, siqueira@sc.usp.br).

Abstract: This paper deals with impedance control of a rotary Series Elastic Actuator designed to assist in flexion/extension of the knee joint during physical therapy. The device includes a DC motor, a worm gear and a customized torsion spring. Since the elastic element is the most important component in the actuator design, a finite element analysis is used to meet the specific requirements of knee assistance. The proposed impedance control scheme comprises three cascade controllers: an inner-loop PI velocity controller, a PI torque controller, and an outer-loop PD position controller. The impedance controller's performance is evaluated through the Frequency Response Function analysis, and experimental results demonstrate the ability of the system to reproduce impedance behavior within an amplitude and frequency range compatible for gait assistance.

Keywords: rehabilitation robotics, active knee orthosis, series elastic actuator, torsion spring, impedance control.

1. INTRODUCTION

The use of robotic devices for rehabilitation of neurological patients is rapidly increasing due to the importance of functional exercises to stimulate motor cortex and improve motor recovery, Ferris et al. (2006). Studies proved that rehabilitation of post-stroke patients was intensified with robot-assisted therapy, Prange et al. (2006); Kwakkel et al. (2008). The advantages of robotic therapy compared with traditional ones also include the ability to evaluate patient progress constantly through objective measures, and the possibility of customizing the treatment according to the patient's level of commitment.

In general, robotic therapy includes a combination of exercises involving passive, active-assisted or active-resisted movements. This combination of exercises can be obtained through the implementation of impedance control, proposed in Hogan (1985), which allows adjustment of the level of interaction between the device and the patient. For example, support torque can be provided by an active orthosis only when needed during gait training. During the rest of the gait, the orthosis should take a low impedance behavior, so as to be fully complacent with the patient's actions. The impedance control can also be used to impose a controlled resistance to the movement of the patient aiming to strengthen muscle groups.

According to Sergi et al. (2012), traditional stiff and high-precision actuators are being replaced by systems with intrinsic compliance in devices where human-robot interaction is present. Traditional stiff actuators are not suitable for such a systems because they cannot achieve low mechanical impedance comparable to those of human joints.

This work considers the Series Elastic Actuator (SEA) concept proposed by Pratt and Williamson (1995), where elasticity is intentionally introduced in series between the gear-motor and the load. This configuration decouples the gear-motor inertia and other nonlinearities from the output and isolates the drivetrain from shocks introduced by the load. Also, the elastic element can be used as a torque sensor, considering the linear relationship between spring deflection and torque. However, there are no commercially available and sufficiently compact rotary compliant components able to simultaneously fulfill both torque and stiffness requirements for rehabilitation.

Two solutions are commonly adopted for the elastic element design: low stiffness arrangement of linear springs, Yoon et al. (2005); Tsagarakis et al. (2009), and the development of customized elastic element, Lagoda et al. (2010); Carpino et al. (2012). The second approach overcomes some problems like residual deflection, hysteresis and a non-linear behavior in the torque versus angle relationship generally present at the first one. These problems compromise accurate torque estimation and, consequently, control performance.

This paper presents a new rotary SEA, where a customized torsion spring is proposed. The torsion spring is obtained through simulation based on Finite Element Method (FEM) to satisfy the specific requirements of knee assistance. Impedance controller is implemented to ensure safe interaction with the patient and enable new strategies for rehabilitation.

⋆ This work was supported by São Paulo Research Foundation (FAPESP) under grant n^o 2011/04074-3.

This paper is organized as follows: Section 2 describes the design requirements and the mechanical design of both SEA and customized torsion spring; Section 3 presents the results of the implementation of impedance controller and Section 4 presents the discussions and conclusions.

2. MECHANICAL DESIGN

2.1 Design Requirements

In this section, it is presented the design process of the SEA, including the customized torsion spring characterization. Considering that the maximum power exerted by the knee joint is 0.739 W/kg, with a maximum torque of 0.365 Nm/kg, and that active knee orthosis should be able to supply 60 % of the peak torque from the gait pattern of a healthy person with approximately 70 kg, the new robotic device must provide a torque assistance up to than 15 Nm. Regarding that more than 95 % of the Power Spectral Density (PSD) of the knee joint torque is in the frequency range between 0 and 5 Hz a minimum torque bandwith of 5 Hz is defined as a requirement to torque control. These design requirements were based on gait data described in Kirtley (2006).

The elastic element is the most important component in the design of a SEA, therefore it must be carefully designed. According to Robinson et al. (1999) the higher the spring constant value, the greater the torque bandwidth. However, low impedance and stiction need that the spring constant be as low as possible. Hence, the elastic constant is defined considering the minimum torque bandwidth taking into account that low impedance and stiction are desired. The constant spring to assist movement of the knee usually lies in the range from 100 to 300 Nm/rad, Sergi et al. (2012). A stiffness of 200 Nm/rad is defined as target value for the design. This was achieved through theoretical analysis considering the desired torque bandwidth, following the procedures described in Robinson (2000).

2.2 Selection of Motor and Gear Reducer

The mechanical design was conceived in order to obtain a compact and lightweight architecture. All housing parts were made of aluminium for the purpose of reduced weight. The final assembly of the rotary SEA consists of a) Maxon Motor RE 40, graphite brushes, 150 Watt DC motor, b) worm gear set (M1-150 of HPC Gears International Ltd.) with reduction ratio of 150:1, c) customized torsion spring, d) angular contact bearings, e) magneto-resistant incremental encoder, and f) opto-electronic incremental encoder. The overall dimensions are shown in Fig.1 and the resulting mass is 2.53 kg, allowing direct mounting of the actuator on the frame of a knee orthosis.

The choice of gear-motor was made based on the characteristics of the knee joint considering of gait pattern of a healthy person. The angular velocities of the knee joint are in the range of +/- 50 rpm and the maximum required torque is 15 Nm, while the maximum continuous torque and the maximum speed of the selected motor are respectively 0.181 Nm and 8200 rpm. Therefore a worm gear set with reduction ratio of 150:1 is used to adjust the operating range of motor in order to fulfill the

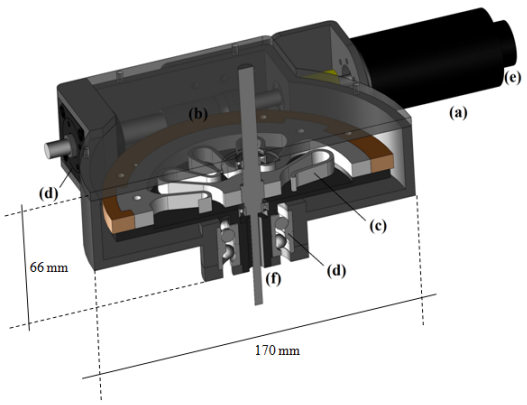

Fig. 1. Cross section of the rotary SEA showing drivetrain components

requirements for velocity and torque. Thereby the worm gear output can operate in a velocities range of +/- 55 rpm and, if the efficiency of the gears is not considered, can provide a maximum continuous torque of 27.15 Nm. However, the friction between the gear significantly reduces the efficiency and the torque amplification ratio is not necessarily the same as the ratio speed reduction, Kong et al. (2012). For this reason, a safety factor of 1.8 to the torque requirement is considered.

All relevant information to the control system, i.e. motor rotation, actuator output, and spring deflection estimate, are obtained by two encoders. A magneto-resistant incremental encoder with a resolution of 4096 pulses per revolution in quadrature decoding mode is used to measure the motor rotation and allows to estimate the position of the worm wheel and a opto-electronic incremental encoder with a resolution of 2000 pulses per revolution in quadrature decoding mode is used to measure the actuator output. The spring deflection estimate is obtained by the difference between the position of the worm wheel and the actuator output. The theoretical output torque resolution is given by $k_s(2\pi/2000)$, where k_s is the spring constant.

2.3 Customized Torsion Spring

To meet the requirements of the proposed application the elastic element should be compact, lightweight, and able to withstand high torque with low intrinsic stiffness. However, this characteristics are not found in commercially available torsion springs. For this reason, a new topology torsion spring was developed. Figure 2 shows perspective view of the torsion spring. It is composed of two rings interconnected by flexible elements. The shape and size of the flexible elements were defined by finite element analysis, see Santos et al. (2013) for details. The material selected for analysis and fabrication was chromium-vanadium steel (AISI 6150), with a Young's modulus of 205 GPa and a yield strength of approximately 1320 MPa after a heat treatment process.

The customized torsion spring, shown in Fig. 2, has been manufactured using the Wire Electrical Discharge Machining (WEDM) process. The mass of the spring is 0.384 kg with a thickness of 8 mm and maximum diameter of 125 mm.

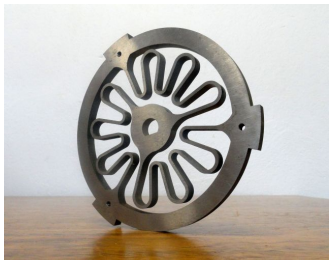

Fig. 2. Customized torsion spring

Experimental characterization of the spring stiffness was performed by coupling on the output shaft of the SEA in a torque sensor (Gamma SI-65-5 from ATI Industrial Automation, Inc.). The SEA was programmed to follow a position profile consisting of a sequence of steps (amplitude 0.14 deg, duration 10 sec) in both loading and unloading conditions, while the torque was measured by the sensor. Figure 3 shows the obtained results.

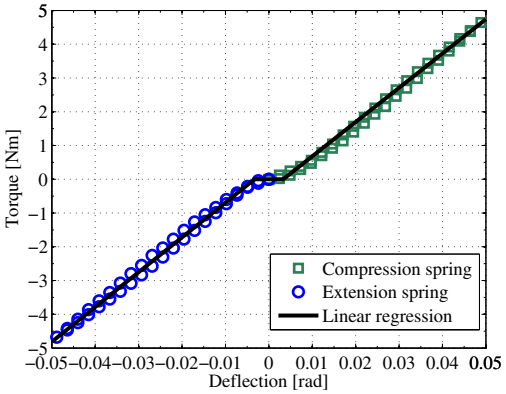

Fig. 3. Characterization of the customized torsion spring

It is possible to observe a non-negligible backlash with an amplitude of approximately 0.0088 rad occasioned by intrinsic feature of the worm gear set. A linear regression was performed in both directions (compression and extension). When the spring is compressed (positive deflection), the stiffness is equal to 106 Nm/rad, when it is extended (negative deflection), the stiffness is equal to 103 Nm/rad. The value of the spring constant determined experimentally is approximately 50 % lower than the obtained by finite element analysis. This discrepancy is probably due to the actual properties of the material being different from the nominal used in the simulation. The final assembly of the rotary SEA and a preliminary setup of a knee orthosis with the rotary SEA attached to it are shown in Figs. 4 and 5, respectively.

Fig. 4. Rotary Series Elastic Actuator

Fig. 5. Rotary SEA attached to a knee orthosis

3. IMPEDANCE CONTROL

This section presents the impedance control design and characterization. The control hardware consists of a EPOS 24/5 Positioning Controller manufactured by Maxon Motor and an ordinary computer hardware equipped with a CAN communication card manufactured by National Instruments. The EPOS is a full digital smart motion controller capable of operating in position, velocity and current modes. The device also is responsible to decode the signals from quadrature encoders. The communication interface between the computer hardware and the EPOS controller is performed by CANopen communication protocol. The frequency of the control-loop is set at 200 Hz.

3.1 Control scheme

The block diagram of the proposed impedance control loop is illustrated in Fig. 6. The control strategy involves three cascade controllers: an inner PI velocity controller, a PI torque controller that generates the desired velocity, $\dot{\theta}_{m,d}$, to the inner loop, and a PD position controller used as an external control loop. The external position controller determines the desired torque, $\tau_{L,d}$, according to position and velocity errors and impedance parameters. Thus, the desired torque can be expressed by:

$$\tau_{L,d} = k_v(\theta_{L,d} - \theta_L) + b_v(\dot{\theta}_{L,d} - \dot{\theta}_L), \tag{1}$$

where k_v and b_v are the virtual stiffness and damping parameters.

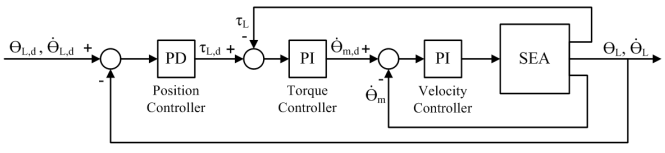

Fig. 6. Block diagram of the impedance control scheme

In the adopted approach, the motor is treated as a velocity source. According to Robinson (2000); Wyeth (2006) this approach helps to overcome some undesirable effects of the gear-motor such as static and dynamic friction intrinsic to the drivetrain. The inner velocity loop was performed

by the built-in EPOS velocity control and the controller parameters were automatically determined by the device. The torque and impedance controllers were implemented through the programming interface Microsoft Visual Studio in the computer hardware. The torque control strategy adopted allows the rotary SEA provide a continuous torque of 5 Nm with a bandwidth of 9.4 Hz. However, this paper deals only with the implementation of the impedance control, the performance of torque control is discussed in Santos et al. (2013).

As a preliminary validation, the SEA was commanded to track a knee joint trajectory profile, for a gait cycle duration of 1.1 s, to evaluate the ability of SEA to reproduce the trajectory of a healthy person without changing the speed of walking. The controller parameters were adjusted to $k_v = 90$ Nm/rad and $b_v = 0$ Nms/rad. The SEA follows the reference trajectory with a delay of approximately 60 ms.

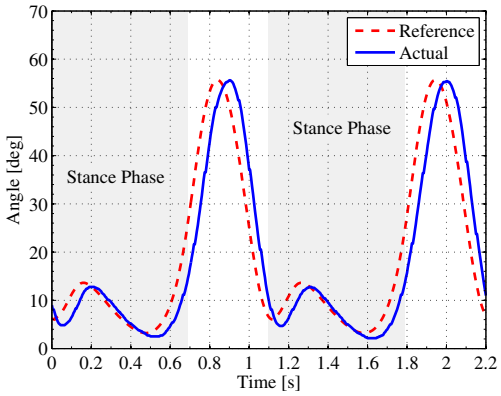

Fig. 7. SEA tracking a typical knee trajectory profile

3.2 Experimental characterization

The characterization of impedance control was performed through the Frequency Response Function (FRF) analysis, obtained by means of the $H_1(\omega)$ and $H_2(\omega)$ estimators, proposed in Maia and Silva (1997). The estimator $H_1(\omega)$ considers the presence of random noise in the output signal, and in this case, the FRF is calculated as, $H_1(\omega) = S_{XY}(\omega)/S_{XX}(\omega)$, being $S_{XY}(\omega)$ the cross-spectrum of the input and output signal, and $S_{XX}(\omega)$ the auto-spectrum of the input signal; the estimator $H_2(\omega)$ considers the presence of random noise in the input signal, and in this case, the FRF is calculated as, $H_2(\omega) = S_{YY}(\omega)/S_{XY}(\omega)$, being $S_{YY}(\omega)$ the auto-spectrum of the output signal. The results obtained by estimators can be evaluated through the ordinary coherence function $C(\omega)$ defined as the ratio of the $H_1(\omega)$ estimator over the $H_2(\omega)$ estimator. The ordinary coherence function is always a real value between 0 and 1 where a value near to 1 represents a good estimate of both estimators.

Two experiments were conducted in order to evaluate the ability of SEA to reproduce the behavior of the knee joint impedance within a frequency range suitable for the given application. First, considering a pure damping control through transfer function $\mathrm{Z}(\omega) = \mathrm{T}(\omega)/\Omega(\omega)$, where $\mathrm{T}(\omega)$ and $\Omega(\omega)$ are the frequency-domain representation of τ_L and $\dot{\theta}_L$, respectively. In the second experiment, considering a pure stiffness control through transfer function $\mathrm{Y}(\omega) = \mathrm{T}(\omega)/\Theta(\omega)$, where $\Theta(\omega)$ is the frequency-domain representation of θ_L. The input signals used to estimate the FRF in both experiments were generated by a human operator by imposing oscillating movements to the SEA output shaft. The average values of the peak torque applied to the output shaft for analysis of the damping and stiffness control were 7 and 3 Nm respectively.

Damping control The pure damping control was obtained, by setting $\dot{\theta}_{L,d} = 0$ and $k_v = 0$, and evaluated varying the value of b_v in 5, 10 and 15 Nms/rad. Figure 8 shows the Bode plot of the closed loop transfer function $\mathrm{Z}(\omega)$, computed from the estimators, and the coherence function between the signals. The damping control bandwidth is approximately 3 Hz and no significant variations in bandwidth were observed for the different values of b_v. However, a difference of 3 Nms/rad was evidenced between the desired value of b_v and the actual, demonstrating the existence of an intrinsic damping in the system.

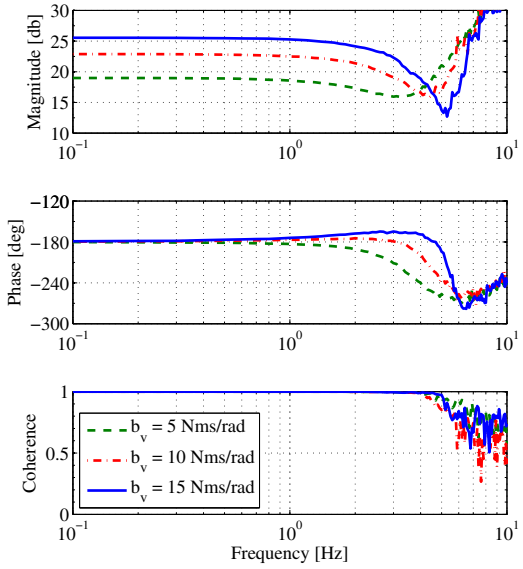

Fig. 8. Damping control response frequency

Stiffness control Similarly to the first experiment, the pure stiffness control was obtained, by setting $\theta_{L,d} = 0$ and $b_v = 0$, and evaluated varying the value of k_v in 10, 30 and 60 Nm/rad. Figure 9 shows the Bode plot of the closed loop transfer function $\mathrm{Y}(\omega)$, computed from the estimators, and the coherence function between the signals. The stiffness control bandwidth considering the values k_v equal to 10, 30 and 60 Nm/rad are respectively 0.4, 1.3 and 2.6 Hz. Note that a larger bandwidth is achieved with higher values of k_v. This is justifiable, since the largest bandwidth is obtained when k_v is equal to k_s (approximately 105 Nm/rad), and at high frequencies, the virtual stiffness value, k_v, tends to spring stiffness, k_s.

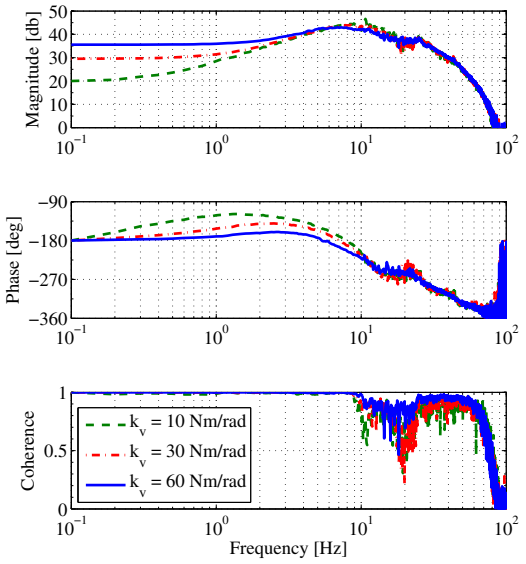

Fig. 9. Stiffness control response frequency

3.3 Variable impedance control strategy

In order to evaluate the variable impedance control strategy applied to the proposed SEA, two discrete impedance parameters for each phase of the gait cycle, stance and swing, were defined as: K_1 and K_2 that represents, respectively, a virtual stiffness of 90 and 20 Nm/rad. In both cases, the virtual damping was set to zero. The SEA was commanded to track a knee trajectory profile computed by interpolation of several points of a normal gait obtained in Kirtley (2006), for a gait cycle duration of 4.4 s, Fig 10.

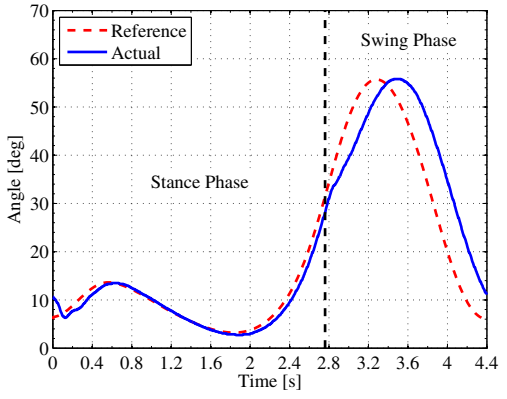

(a) Variable impedance without external torque

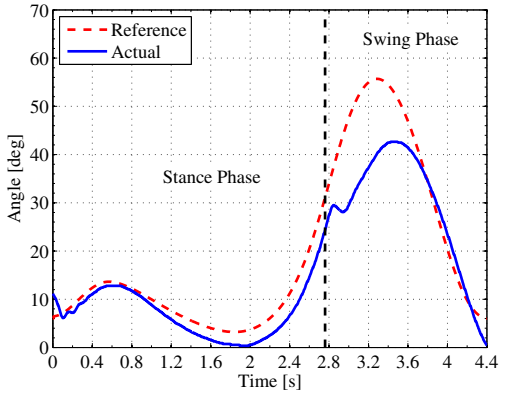

(b) Variable impedance with external torque applied

Fig. 10. Analysis of the variable impedance control

Figure 10(a) show the SEA behavior in the absence of external torque. In other words, when there is no movement restriction. It is possible to note that the reference trajectory is followed by the SEA in the two different impedance states (K_1 and K_2). On the other hand, when a torque is applied against the desired trajectory, Fig. 10(b), the reference trajectory is followed only in the highest impedance state, K1. In this case, the applied torque by the SEA compensates the external torque and guarantees the trajectory tracking. However, in the low impedance state, K_2, the torque decreases and the reference trajectory is not followed, allowing the user to move the SEA easily out of the desired trajectory.

4. CONCLUSIONS

This paper presents the impedance control characterization of a rotary Series Elastic Actuator (SEA) designed for knee rehabilitation. A customized torsion spring is designed and evaluated, resulting in a stiffness constant suitable to assist movement of the knee joint. The resulting mass of the SEA is 2.53 kg, thus allowing direct mounting of the actuator on the frame of a knee orthosis. Impedance controller is implemented to ensure secure interaction with the patient, enabling new strategies for rehabilitation. For example, a variable impedance control strategy is performed and shows that it is possible to regulate the impedance during walking. Also, the performance of the impedance control scheme is characterized experimentally using system identification techniques, and he results show that the actuator is able to reproduce impedance behavior within an amplitude and frequency range appropriate to assist the knee joint.

REFERENCES

Carpino, G., Accoto, D., Sergi, F., Tagliamonte, N.L., and Guglielmelli, E. (2012). A novel compact torsional spring for series elastic actuators for assistive wearable robots. *Journal of Mechanical Design*, 134, 1–10.

Ferris, D.P., Sawicki, G.S., and Domingo, A. (2006). Powered lower limb orthoses for gait rehabilitation. *Topics in Spinal Cord Injury Rehabilitation*, 11(2), 34–49.

Hogan, N. (1985). Impedance control: an approach to manipulation. *Journal of Dynamic Systems Measure Control*, 107(Parts 1-3)(1), 1–24.

Kirtley, C. (2006). *Clinical Gait Analysis: Theory and Practice*. Elsevier Churchill Livingstone, 1st edition edition.

Kong, K., Bae, J., and Tomizuka, M. (2012). A compact rotary series elastic actuator for human assistive systems. *IEEE/ASME Transactions on Mechatronics*, 17(2), 288–297.

Kwakkel, G., Kollen, B.J., and Krebs, H.I. (2008). Effects of robot-assisted therapy on upper limb recovery after stroke: A systematic review. *Neurorehabilitation and Neural Repair*, 22(2), 111–121.

Lagoda, C., Schouten, A., Stienen, A., Hekman, E., and van der Kooij, H. (2010). Design of an electric series elastic actuated joint for robotic gait rehabilitation training. In *Proceedings of 3rd IEEE RAS and EMBS International Conference on Biomedical Robotics and Biomechatronics*, 21–26. Tokyo, Japan.

Maia, N. and Silva, J. (1997). *Theoretical and Experimental Modal Analysis*. Engineering dynamics series. Research Studies Press Limited.

Prange, G.B., Jannink, M.J.A., Groothuis-Oudshoorn, C.G.M., Hermens, H.J., and Ijzerman, M.J. (2006). Systematic review of the effect of robot-aided therapy on recovery of the hemiparetic arm after stroke. *Journal of Rehabilitation Research and Development*, 43(2), 171–183.

Pratt, G. and Williamson, M. (1995). Series elastic actuators. In *Proceedings of the 1995 IEEE/RSJ International Conference on Intelligent Robots and Systems*, volume 1, 399–406. Pittsburgh, USA.

Robinson, D.W. (2000). *Design and Analysis of Series Elasticity in Closed-loop Actuator Force Control*. Ph.D. thesis, Massachusetts Institute of Technology, Cambridge.

Robinson, D.W., Pratt, J.E., Paluska, D.J., and Pratt, G.A. (1999). Series elastic actuator development for a biomimetic walking robot. In *IEEE/ASME International Conference on Advanced Intelligent Mechatronics*, 561–568.

Santos, W.M., Caurin, G.A.P., and Siqueira, A.A.G. (2013). Torque control characterization of a rotary series elastic actuator for knee rehabilitation. In *16th International Conference on Advanced Robotics*. Montevideo, Uruguay.

Sergi, F., Accoto, D., Carpino, G., Tagliamonte, N.L., and Guglielmelli, E. (2012). Design and characterization of a compact rotary series elastic actuator for knee assistance during overground walking. In *The Fourth IEEE RAS/EMBS International Conference on Biomedical Robotics and Biomechatronics*, 1931–1936. Roma, Italy.

Tsagarakis, N., Laffranchi, M., Vanderborght, B., and Caldwell, D. (2009). A compact soft actuator unit for small scale human friendly robots. In *Proceedings of IEEE International Conference on Robotics and Automation*, 4356–4362. Kobe, Japan.

Wyeth, G. (2006). Control issues for velocity sourced series elastic actuators. In *Proceedings of the Australasian Conference on Robotics and Automation*. Auckland, New Zealand.

Yoon, S.S., Kang, S., Yun, S.K., Kim, S.J., Kim, Y.H., and Kim, M. (2005). Safe arm design with mr-based passive compliant joints and viscoelastic covering for service robot applications. *Journal of Mechanical Science and Technology*, 19(10), 1835–1845.